*International Journal of Engineering & Technology*, 7 (3.7) (2018) 315-319

**International Journal of Engineering & Technology**

*Website: www.sciencepubco.com/index.php/IJET*

***Research paper***

# Supercontinuum Generated Micro-structured Fibre for Optical Communications and Medical Applications

**Feroza Begum[1,*], Pg Emeroylariffion Abas[1], Iskandar Petra[1], Shubi Felix Kaijage[2] and Nianyu Zou[3]**

[1]*Faculty of Integrated Technologies, Universiti Brunei Darussalam, Jalan Tungku Link, Gadong BE 1410, Brunei Darussalam*
[2]*School of Computational and Communication Science and Engineering, Nelson Mandela African Institution of Science and Technology, Arusha, Tanzania.*
[3]*School of Information Science and Engineering, Dalian Polytechnic University, Dalian, China*
**Corresponding author E-mail: feroza.begum@ubd.edu.bn*

## Abstract

This paper proposes a simple highly nonlinear photonic crystal fibre (HN-PCF) for generating supercontinuum (SC) spectrum in telecommunication window. Hexagonal structured HN-PCF with two different air hole diameters was modelled for numerical simulation and various properties of proposed photonic crystal fibres were calculated using finite difference method, and analysed. It has been demonstrated that nonlinear coefficients values of 113 $[Wkm]^{-1}$ at 1.0 μm, 71 $[Wkm]^{-1}$ at 1.30 μm and 51 $[Wkm]^{-1}$ at 1.55 μm are obtainable; with flattened chromatic dispersion. The remarkably low confinement loss of less than $10^{-5}$ dB/km is obtainable in the wavelength range of between 1.0 μm and 1.7 μm. Moreover, it has been shown that it is possible to generate wide SC spectrum using 1.0 ps input pulses to achieve longitudinal resolution of 1.5 μm and 1.1 μm at 1.06 μm and 1.31 μm centre wavelengths, respectively. This proposed HN-PCF may be applicable for supercontinuum spectrum generation and all-optical signal processing in the infrared region.

***Keywords***: *Photonic Crystal Fibre; Chromatic Dispersion; Confinement Loss; Supercontinuum Spectrum*

## 1. Introduction

Index-guiding photonic crystal fibres (PCFs) or micro structured fibres have attracted considerable attention from the optical community [1] due to its interesting properties. Periodicity of the cladding area in index-guiding PCF is not essential for the confinement of the guiding light onto the core. Therefore, dispersion and dispersion slope of the fibre may be controlled by changing cladding structure, air holes' size, and pitch distance between two adjacent air holes, in wide wavelength range. PCFs have exhibited remarkable dispersion and leakage properties [1, 2] and have been shown to a good candidate for generating supercontinuum (SC) spectrum [3, 4].

To date, different index-guiding highly nonlinear PCFs (HN-PCFs) and semiconductor diode have been reported for SC generation in the telecommunication window and for medical applications [5–11]. Reference [5] reports an HN-PCF [5] with nonlinear coefficients of around 30 $W^{-1}km^{-1}$ at the 1.55 μm wavelength, however, the design is relatively complex; having four to five different air hole diameters.

Wavelengths near the 1.0 μm and 1.3 μm values are especially attractive in ophthalmology and dentistry, respectively. Images from Optical Coherence Tomography (OCT) using the wavelengths exhibits favourable properties; showing deeper penetration and improved sensitivity with minimal dispersion. Commonly, super-luminescent diodes (SLDs) [6, 7] and femtosecond laser sources [8–11] are used as light sources in OCT and optical communication. SLDs are able to produce longitudinal resolution of 10-15 μm that are required in standard OCT applications. To improve the resolution even further such that identification of individual cell is possible, femtosecond based light sources may be used. However, its usage in OCT system is limited, due to its prohibitively high cost. As such, the search is still on; to produce affordable ultra-high resolution OCT systems, with the relatively less expensive picosecond pulse laser sources widely viewed as potential light source in OCT system.

This paper proposes a simple HN-PCF structure for SC generation with ultra-high longitudinal resolution for the telecommunication window and medical application. It is shown, via numerical simulation, that the proposed seven-ring HN-PCF exhibits ultra-flattened chromatic dispersion and very low confinement loss, with high non-linear coefficient value. Moreover, the proposed fibre is capable of generating 225 nm, 412 nm and 440 nm wide full width half maxima (FWHM) SC spectrum at 1.06 μm, 1.31 μm and 1.55 μm centre wavelengths, respectively. Longitudinal resolutions of 1.5 μm and 1.1 μm at 1.06 μm and 1.31 μm centre wavelength, respectively, are obtainable using the proposed fibre.

## 2. Proposed HN-PCF diagram

Schematic design of the proposed HN-PCF is shown in Figure 1. It is made up of seven air hole rings; with two air holes sizes of diameter $d_1$ and $d$, and pitch $\Lambda$. The host material is regular silica. Diameters of air holes on the first and fourth rings are reduced; in order to manipulate dispersion characteristics of the fibre, whilst maintaining sufficiently large diameter of the other air holes for better field confinement.

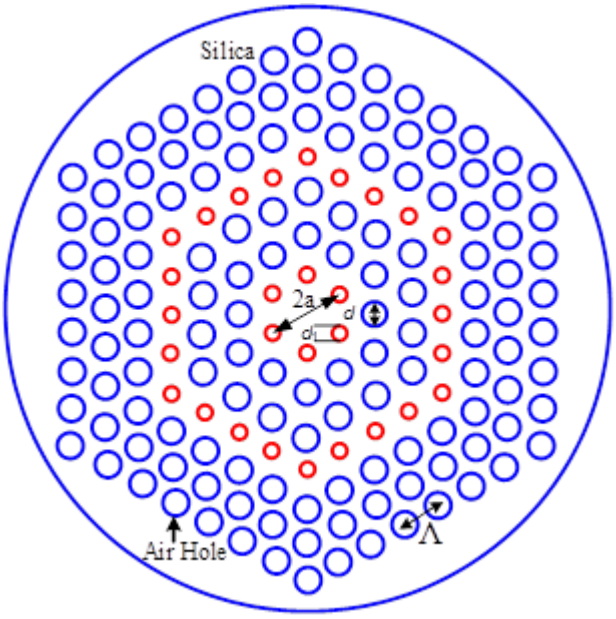


**Figure 1:** Schematic design of the proposed HN-PCF.

## 3. Numerical method

The proposed fibre is analysed using Finite Difference Method (FDM) with anisotropic Perfectly Matched boundary Layer (PML). In particular, properties of interest are chromatic dispersion $D(\lambda)$, dispersion slope $D_s$, confinement loss $L_c$, effective area $A_{eff}$ [12] and nonlinear coefficient $\gamma$ [13].

Modal effective refractive indices $n_{eff}$ of the fibre may be derived by solving eigenvalue problem which is drawn from Maxwell's equations, using the FDM. The above properties may then be calculated using the following equations; obtained from references [12] and [13]:

$$D = -\frac{\lambda}{c}\frac{d^2 R_e(n_{eff})}{d\lambda^2} \quad (1)$$

$$D_s = \frac{\partial D(\lambda)}{\partial \lambda} \quad (2)$$

$$L_C = \frac{2\times 10^7}{\ln(10)}\frac{2\pi}{\lambda}\mathrm{Im}(n_{eff}) \quad (3)$$

$$A_{eff} = \frac{2\pi\left(\int_0^\infty |E_a(r)^2| r dr\right)^2}{\int_0^\infty |E_a(r)|^4 r dr} \quad (4)$$

$$\gamma = \frac{2\pi n_2}{\lambda A_{eff}} \quad (5)$$

Where, $\lambda$ is the operating wavelength, Re($n_{eff}$) and Im($n_{eff}$) are real and imaginary parts of the modal effective refractive index, c is the velocity of light in vacuum, $E$ is the electric field and $n_2$ is the nonlinear refractive index coefficient. $d(.)/d\lambda$ and $d^2(.)/d\lambda^2$ represent first and second differential with respect to the operating wavelength.

## 4. Simulation Results

For simulation and analysis, diameter of air holes is fixed at $d$ = 0.78 µm, with diameter of air holes on the first and fourth rings reduced to $d_1$ = 0.32 µm. Distance between air holes is fixed at Λ = 0.87 µm. Wavelength dependent properties of the proposed HN-PCF are shown in Figure 2.

Figure 2 (a) shows relationships between dispersion properties of the proposed fibre and operating wavelength. It can be seen that the fibre exhibits ultra-flattened chromatic dispersion, with values between 0 ps/(nm.km) and – 8 ps/(nm.km) at operating wavelength range from 1.0 µm to 1.7 µm; to give variable chromatic dispersion slope between ± 0.06 ps/(nm$^2$.km). The small dispersion slope offers the possibility of smaller pulse broadening for the wide bandwidth ranges. Confinement loss of less than $10^{-5}$ dB/km over the operating wavelengths under consideration, may be expected, as shown in Figure 2 (b). As depicted in Figure 2 (c), effective areas at operating wavelengths of 1.0 µm, 1.3 µm and 1.55 µm are 1.72 µm$^2$, 2.11 µm$^2$ and 2.44 µm$^2$, respectively; comparatively smaller to that of conventional fibres with effective area of approximately 86 µm$^2$ at the 1.55 µm wavelength. These give corresponding nonlinear coefficients of 113 [Wkm]$^{-1}$, 71 [Wkm]$^{-1}$ and 51 [Wkm]$^{-1}$ at 1.0 µm, 1.30 µm and 1.55 µm operating wavelengths, respectively. Nonlinear coefficients of the proposed fibre are higher than other fibres in references [4, 5].

Next, the effect of reducing diameter of air holes on the fourth ring is investigated. Figure 3 (a) shows the wavelength dependence properties of two fibres; 1) the proposed fibre in Figure 1, with diameter of air holes on the first and fourth rings reduced to $d_1$ whilst diameter of the rest of the air holes fixed at $d$ (referred to as the Optimum), and 2) the proposed fibre in Fig. 1, but with diameter of air holes on only the first ring reduced to $d_1$ whilst diameter of the rest of the air holes fixed at $d$. Parameters of the fibres are $d_1$ = 0.32 µm, $d$ = 0.78 µm, and Λ = 0.87 µm. It can be seen from the figure that fourth ring diameter has an influence on dispersion properties of the fibre. Reducing diameter of air holes on the first ring only shift the dispersion curve downwards, as compared to the proposed fibre in Figure 1. As such, appropriate pitch and air hole diameter selections are very important to obtain flat and zero dispersion; favourable property for HN-PCF for the telecommunication window.

During fabrication of a standard fibre, it is expected that ± 2% variations may occur in the diameter of air holes of the first ring [14]. Due to this, it is important to analyse the effect of these variations on important properties of the fibre; to pre-empt the characteristics of the fibre after fabrication. Figure 3 (b) and (c) depict the effect of variations (± 5% variations) on the first ring air hole diameter $d_1$, on the chromatic dispersion and effective area of the proposed fibre, respectively. Dotted line indicates increased diameter by +5% whilst dashed line indicates decreased diameter by -5%.

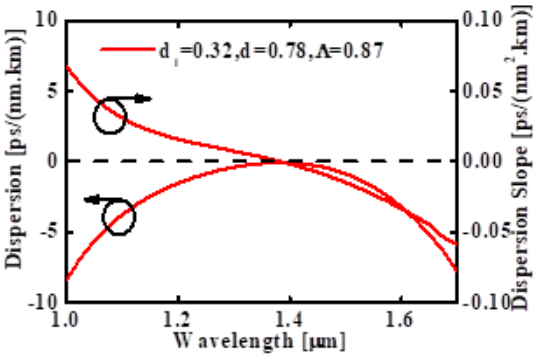


(a)

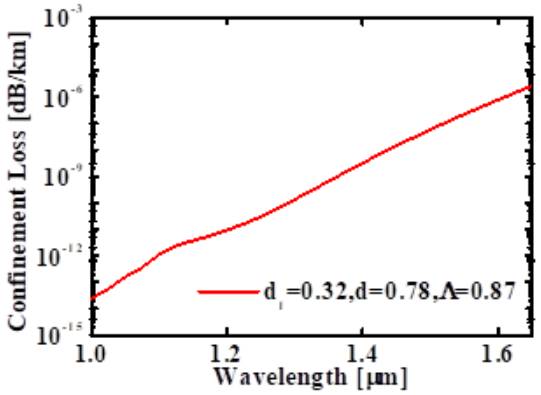


(b)

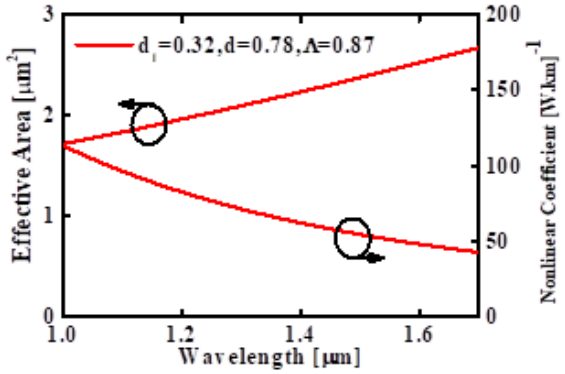


(c)

**Figure 2:** (a) Chromatic dispersion and chromatic dispersion slope, (b) confinement loss and (c) effective area and nonlinear coefficient, as a function of wavelength for the proposed HN-PCF in Fig. 1 with Λ = 0.87 μm, $d_1$ = 0.32 μm, $d$ = 0.78 μm.

From the figures, it can be concluded that curves for chromatic dispersion and effective area are shifted slightly downward with an increase in diameter of first ring air holes by +5% whilst the curves are shifted slightly upwards with a decrease of -5%.

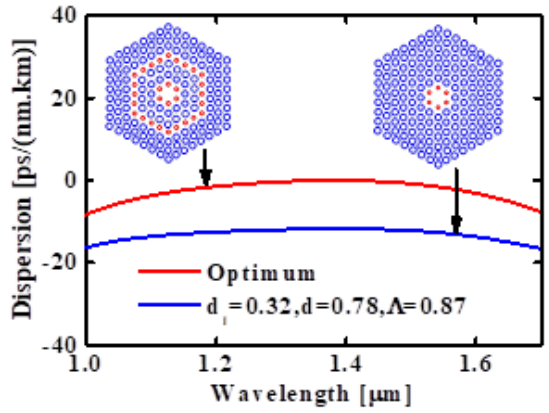


(a)

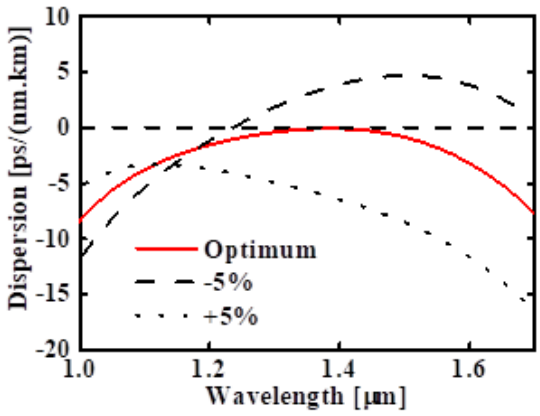


(b)

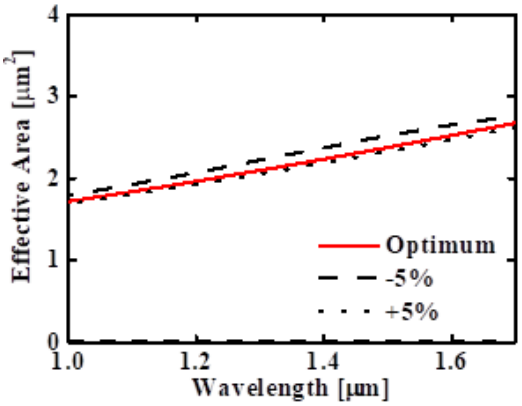


(c)

**Figure 3:** Chromatic dispersion properties to demonstrate (a) the effect of fourth air hole ring diameter, (b) the effect of ± 5% variation of first air hole ring diameters, and (c) effective area to demonstrate the effect of ± 5% variation of first air hole ring diameters, at different operating wavelength for the HN-PCF in Fig. 1 with optimum parameters Λ = 0.87 μm, $d_1$ = 0.32 μm, $d$ = 0.78 μm.

From the result, it can be said that the proposed HN-PCF is able to maintain its desired dispersion property after fabrication.

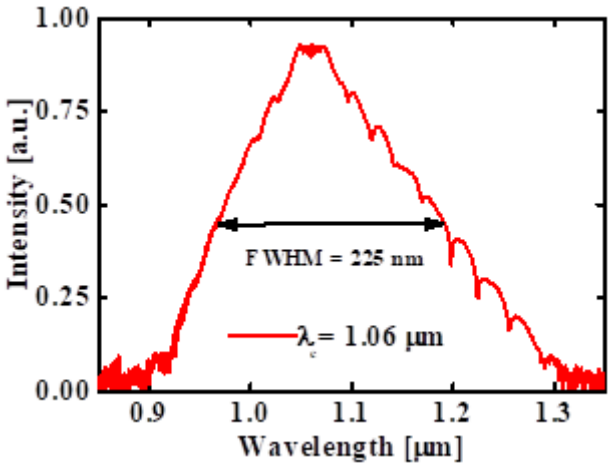


(a)

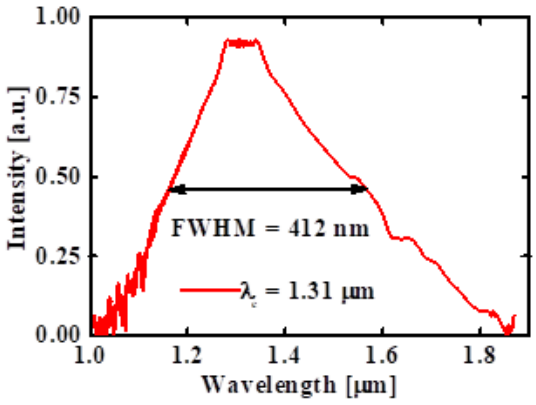


(b)

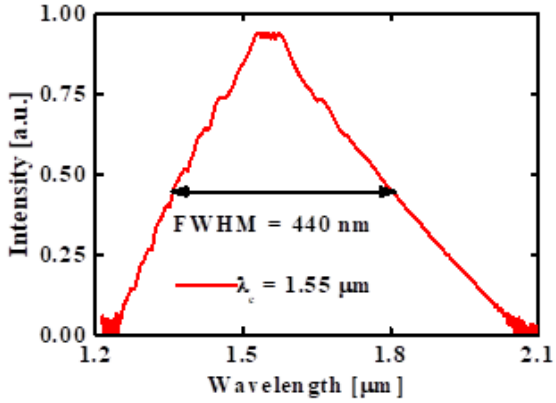


(c)

**Figure 4:** Intensity spectrum of the proposed HN-PCF at centre wavelengths of (a) 1.06 μm, (b) 1.31 μm and (c) 1.55 μm.

## 5. Supercontinuum Spectrum At 1.06 μM, 1.31 μM And 1.55 μM

The following nonlinear Schrödinger equation (NLSE) [13] may be used for calculations of the SC spectrum:

$$\frac{\partial A}{\partial z}+\frac{\alpha}{2}A+\frac{i}{2}\beta_2\frac{\partial^2 A}{\partial T^2}-\frac{1}{6}\beta_3\frac{\partial^3 A}{\partial T^3}= i\gamma\left[|A|^2A+i\frac{\lambda_c}{2\pi c}\frac{\partial}{\partial T}\left(|A|^2A\right)-T_R A\frac{\partial|A|^2}{\partial T}\right] \quad (6)$$

With $T = t - z/v_g$

where $A$ is the complex amplitude of the optical field, $z$ is the propagation distance, $\alpha$ is the absorption coefficient of the fibre, $\lambda_c$ is the centre wavelength, $T_R$ is the slope of the Raman gain, and $\beta_n$ ($n$ =1 to 3) are the $n$-th order propagation constant. Also, $t$ is the physical time and $v_g$ is the group velocity at the centre wavelength.

NLSE may be solved by split-step Fourier method. Supercontinuum generation in the proposed HN-PCF is theritically calculated at 1.06 μm, 1.31 μm and 1.55 μm centre wavelength and shown in Figure 4 (a), (b) and (c), respectively. In Fig. 4, propagation of the sech$^2$ waveform through the proposed HN-PCF is assumed; with the full width at half maximum (FWHM), $T_{FWHM}$ of 1.0 ps and Raman scattering parameter $T_R$ = 3.0 fs. Values of parameters taken for calculation purpose are given in Table 1; where $\beta_2$, $\beta_3$ and $\beta_4$ are propagation constants around the carrier frequency with centre wavelength $\lambda_c$, $L_F$ is fibre length and $P_{in}$ is input power of the incident pulse. The calculated longitudinal resolution $l_r$ and coherent length $l_c$ given in Table 1 assume typical $n_{tissue}$ is 1.44 for eye and 1.65 for dentin, at wavelengths 1.1 μm and 1.31 μm, respectively [15]. It is noted that the calculated $l_r$ values are lower than that of reported SLDs and femtosecond pulse light sources [6 – 11].

**Table. 1:.** Fibre parameters.

| Parameters | $\lambda_c$=1.06 [μm] | $\lambda_c$=1.31 [μm] | $\lambda_c$=1.55 [μm] |
|---|---|---|---|
| $\beta_2$ [ps$^2$/km] | 2.98 | 0.318 | 2.29 |
| $\beta_3$ [ps$^3$/km | 0.01 | 0.0045 | -0.0036 |
| $P_{in}$ [W] | 33.0 | 12.0 | 40 |
| $L_F$ [m] | 8.0 | 50.0 | 12 |
| $l_c$ [μm] | 2.2 | 1.8 | |
| $l_r$ [μm] | 1.5 | 1.1 | |

The influence of input pulse power on output pulse power at centre wavelengths of 1.06 μm, 1.31 μm and 1.55 μm are shown in Fig. 5 (a), (b) and (c), respectively, with the incident pulse full width at half maximum $T_{FWHM}$ = 1.0 ps. From the figure, output pulse power decreases from the peak power of incident pulse, after passing a certain distance; with achieved output pulse power approximately half of the applied input pulse power. Light propagating fibre length $L_F$ are calculated to be 8 m, 50 m and 12 m for centre wavelengths of 1.06 μm, 1.31 μm and 1.55 μm, respectively. All output pulses are selected at different input peak power pulses; input pulse peak power $P_{in}$ of 33 W at 1.06 μm centre wavelength, 12 W at 1.31 μm centre wavelength and 40 W at 1.55 μm centre wavelength.

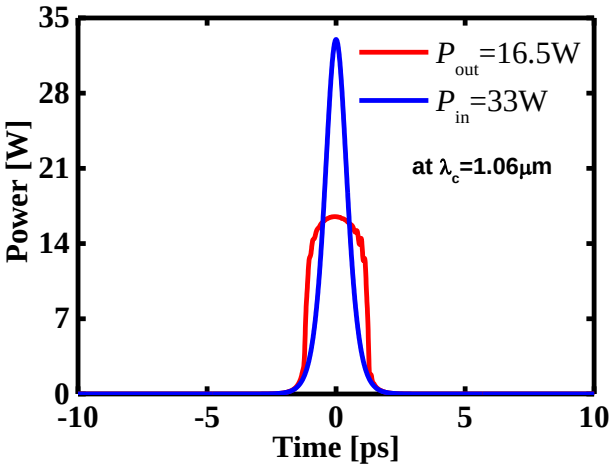


(a)

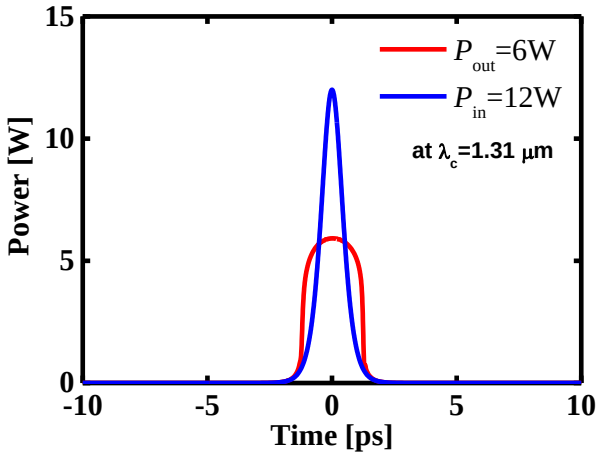


(b)

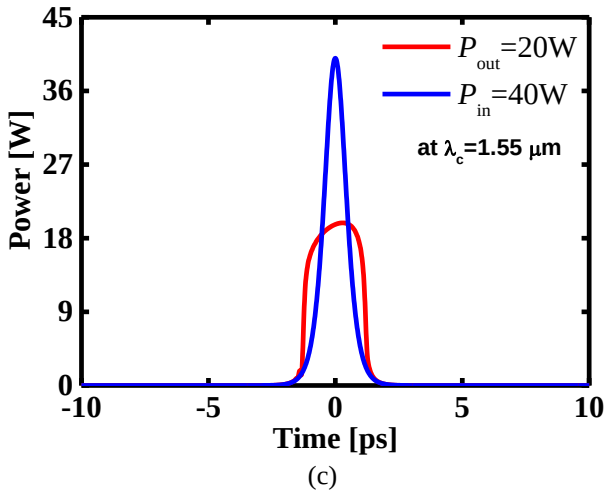


(c)

**Figure 5:** Input and output power optical pulses of the proposed HN-PCF at the centre wavelengths of (a) 1.06 μm, (b) 1.31 μm and (c) 1.55 μm

## 6. Conclusion

In the telecommunication window and for medical applications, simple HN-PCF exhibiting very high nonlinearity, ultra-flattened chromatic dispersion, very low confinement loss and high longitudinal resolution has been designed and analysed. It has been shown that the proposed fibre exhibits chromatic dispersion values of between 0 to – 8.0 ps/(nm.km) in the wavelength range of between 1.0 μm to 1.7 μm; with extremely low confinement loss of less than $10^{-5}$ dB/km. High nonlinear coefficient value of 51 $[Wkm]^{-1}$ is achievable at 1.55 μm wavelength. Moreover, it has been demonstrated that the proposed fibre is able to generate broad SC spectrum, with relatively high longitudinal resolutions of 1.5 μm and 1.1 μm at centre wavelength 1.06 μm and 1.31 μm, respectively. With the mentioned properties, the proposed HN-PCF may be suitable for optical parametric amplification, all-optical signal processing, ultrashort soliton pulse transmission, supercontinuum generation in the infrared region, etc. SC applications include medical imaging, multi-wavelength signal generation, tuneable wavelength conversion, multiplexing format conversion, and optical studies of photonic devices.

## References

[1] Reeves, W. H., et al., Demonstration of ultra-flattened dispersion in photonic crystal fibers. Opt. Express, 2002. 10(14): p. 609-613.
[2] Begum, F., et al., Photonic Crystal Fiber with Ultra-flattened Chromatic Dispersion, Low Confinement and Bending Losses. IEEJ Trans. on Elec. Inform. and Sys., 2009. 129(6): p. 1039-1046.
[3] Begum, F., et. al., Supercontinuum generation in square photonic crystal fiber with nearly zero ultra-flattened chromatic dispersion and fabrication tolerance analysis. Opt. Comm., 2011. 284(4): p. 965-970.
[4] Yamamoto, T., et al., Supercontinuum generation at 1.55 μm in a dispersion-flattened polarization- maintaining photonic crystal fiber. Opt. Express, 2003. 11(13): p. 1537–1540.
[5] Saitoh, K., et al., Highly nonlinear dispersion-flattened photonic crystal fibers for supercontinuum generation in a telecommunication window. Opt. Express, 2004. 12(10): p. 2027–2032.
[6] Jung, E. J., et al., Spectrally-sampled OCT for sensitivity improvement from limited optical power. Opt. Express, 2008. 16(22): p. 17457-17467,
[7] Shibata, H., et al., Imaging of spectral-domain optical coherence tomography using a superluminescent diode based on InAs quantum dots emitting broadband spectrum with Gaussian-like shape. Japanese Jour. of Appl. Phys., 2015. 54(4S): p. 04DG07-1-04DG07-5.
[8] Calmano, T., et al., Nd:YAG waveguide laser with 1.3 W output power, fabricated by direct femtosecond laser writing. Appl. Phys. B, 2010. 100(1): p. 131–135,
[9] Zaytsev, A., et al., Supercontinuum generation by noise-like pulses transmitted through normally dispersive standard single-mode fibers. Opt. Express, 2013. 21(13): p. 16056-16062.
[10] Aguirre, A. D., et al., Continuum generation in a novel photonic crystal fiber for ultrahigh resolution optical coherence tomography at 800 nm and 1300 nm. Opt. Express, 2006. 14(3): p. 1145-1160,
[11] Namihira, Y., et al., Design of Highly Nonlinear Dispersion Flattened Hexagonal Photonic Crystal Fibers for Dental Optical Coherence Tomography Applications. Opt. Review, 2012. 19(2): pp. 78–81.
[12] Begum, F., et al., Design and analysis of novel highly nonlinear hexagonal photonic crystal fibers with ultra-flattened chromatic dispersion. Opt. Comm., 2009. 282(7): p. 1416-1421.
[13] Agrawal, G., Nonlinear Fiber Optics, 2nd Edition, San Diego, CA, Academic Press, 1995.
[14] Poletti, F., et al., Inverse design and fabrication tolerances of ultra-flattened dispersion holey fibers. Opt. Express, 2005. 13(10), p. 3728– 3736.
[15] Fercher, A. F., et al., Optical coherence tomography-principles and applications. Rep. on Prog. Phys., 2003. 66(2): p. 239-303.